Reduced Leakage Current and Ferroelectric Properties in Nd and Mn Codoped $BiFeO_3$ Thin Films

Takeshi Kawae*, Hisashi Tsuda, and Akiharu Morimoto

Graduate School of Natural Science and Technology, Kanazawa University, Kakuma-machi, Kanazawa 920-1192, Japan

Received February 26, 2008; accepted March 28, 2008; published online April 18, 2008

Polycrystalline $BiFeO_3$ (BFO), Nd-doped (BNF), Mn-doped (BFM), and (Nd,Mn)-codoped $BiFeO_3$ (BNFM) thin films were fabricated on Pt/$SrTiO_3$(100) substrate by pulsed laser deposition. According to the X-ray diffraction analysis and atomic force microscope observation, suppression of impurity phases and improvement of surface morphology were realized in the BNFM film. In the BNFM film, the leakage current was reduced compared with BFO, BNF, and BFM films, and *P–E* hysteresis curves were observed with measurement frequency of 100 Hz at room temperature. The remanent polarization and coercive field were approximately 100 $\mu C/cm^2$ and 250 kV/cm, respectively.

DOI: 10.1143/APEX.1.051601

It is well known that $BiFeO_3$ (BFO) is a famous multiferroic material with Curie temperature of 830 °C and Neel temperature of 370 °C. The BFO thin films have attracted much attention due to their excellent ferro/piezoelectric properties, comparable to those of $Pb(Zr_xTi_{1-x})O_3$ (PZT),[1,2] and thus the BFO is expected as an alternative Pb-free ferro/piezoelectric material. However, the BFO has a serious problem of a large leakage current mainly caused by nonstoichiometric compositions in the BFO.

In the last several years, various techniques for solving this problem such as improvements of growth conditions of films and site-engineering based on the defect chemistry in the films were proposed, and reduced leakage current properties were reported.[3–15] Especially, the site-engineering technique is quite important from industrial aspects because that technique can be applied to most of deposition methods in principle. Recently, Singh *et al.*[14] and Lee and Wu[15] proposed codoped BFO films $(Bi_{1-x}La_x)(Fe_{1-y}Ni_y)O_3$ and $(Bi_{1-x}La_x)(Fe_{1-y}Ti_y)O_3$, respectively, they reported fine electrical properties of codoped BFO film capacitors. Although exact control of complicated composition is required, the codoping technique is much interesting since enhanced electrical properties are expected due to synergetic effect combining the various advantages for each substitution. Hence, in the present study, we propose new combination of Nd for Bi-site and Mn for Fe-site as codoping elements of BFO thin films. Some nonvolatile rare-earth ions such as Nd^{3+} and La^{3+} can be substituted for Bi-site of BFO because radii of these ions are similar to that of Bi^{3+} ion,[8] and the nonvolatile rare-earth ion substitution for volatile Bi^{3+} is expected to suppress the impurity phases, improve the surface morphology and reduce the leakage current in the films.[8–11,14,15] Although the leakage current in the La-doped BFO films is slightly smaller than that in the Nd-doped films, La-doping is liable to cause serious degradations in ferroelectric properties.[8] Therefore, Nd is preferable as a dopant for Bi-site. On the other hand, in the Fe-site substitution of BFO, some transition metal such as Ni, Ti, Cr, and Mn were employed as a dopant.[7,12–15] According to the electrical properties of Fe-site substituted BFO film capacitors, Mn-doping showed remarkable effect to reduce the leakage currents in the high electric field region.[7] In this work, we report the synthesis and characterization of (Nd,Mn)-codoped BFO (BNFM) thin films by comparing with those of pure BFO, Nd-doped BFO (BNF), and Mn-doped BFO (BFM) thin films.

BFO, BNF, BFM, and BNFM thin films were deposited on Pt-coated (100) $SrTiO_3$ (STO) substrates using a conventional pulsed KrF excimer laser deposition (PLD) system. The ceramic targets with metal compositions of $Bi_{1.1}FeO_3$, $(Bi_{1.0}Nd_{0.05})FeO_3$, $Bi_{1.1}(Fe_{0.97}Mn_{0.03})O_3$, and $(Bi_{1.0}Nd_{0.05})(Fe_{0.97}Mn_{0.03})O_3$ were used as ablation targets for BFO, BNF, BFM, and BNFM films, respectively. The films were deposited on the substrate at 600 °C with oxygen pressure of 13.3 Pa. Following the deposition, the films were annealed at 600 °C for 60 min in the oxygen pressure of 2.67 kPa in the same deposition chamber. The thickness of deposited films was approximately 300 nm. To investigate the electrical properties of films, Au top electrodes of 2.025×10^{-5} cm^2 in areas were deposited by thermal evaporation using a metal mask on the film, resulting in metal–insulator–metal (MIM) capacitors.

The crystal structure of the films was determined by X-ray diffraction (XRD) with Cu Kα radiation before the deposition of Au top electrodes. The surface morphologies of the films were studied using atomic force microscope (AFM; Autoprobe-cp, Park Scientific Instruments). The polarizations and leakage current of MIM capacitors were measured using RT-66A ferroelectric test system. All measurements were performed at room temperature (RT).

Figure 1 shows the XRD θ–2θ scanning patterns of the BFO, BNF, BFM, and BNFM films grown on the Pt-coated STO substrate. All films were found to be polycrystalline BFO with (100) and (110) orientations. The notation of the BFO diffraction peaks is based on the psuedocubic system unless otherwise stated. In the case of BFO and BFM films, it can be seen that the impurity phases ($Bi_2Fe_4O_9$ and Fe_2O_3 indicated by symbols in the figure) due to Bi deficiency were detected. On the other hand, the impurity phases were weak or nothing in the BNF and BNFM films as shown in the figure. Thus, to obtain the BFO single phase in the film, it is effective to substitute the Nd ion for the volatile Bi-site of BFO, which is same as those reported in the rare-earth elements substituted BFO films.[8,10]

Figure 2 shows the AFM images of BFO, BNF, BFM, and BNFM films. In the BFO film shown in Fig. 2(a), the grains of approximately 300 to 500 nm in size are grown in the film. With Nd doping, the grain size was reduced to approximately 100 to 300 nm in size, the surface morphology was changed to dense and uniform compared with the

*E-mail address: kawae@ec.t.kanazawa-u.ac.jp

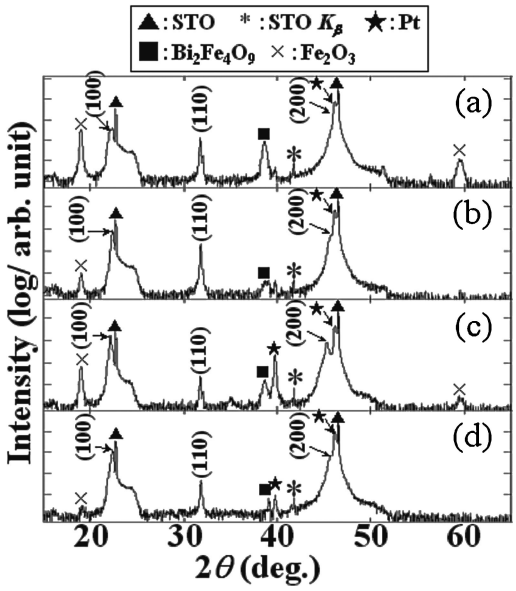

Fig. 1. XRD patterns for (a) BFO, (b) BNF, (c) BFM, and (d) BNFM films grown on Pt coated (100)STO substrate. Symbols indicate the impurity phases and substrate.

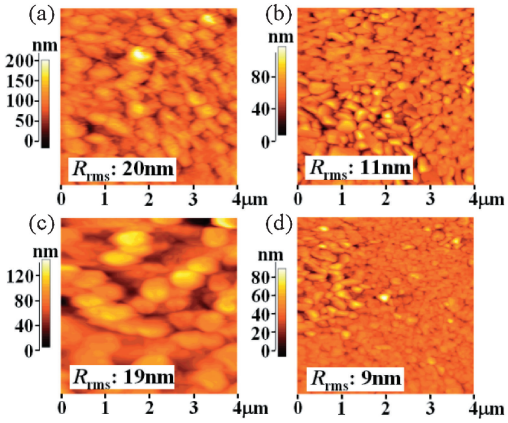

Fig. 2. AFM images for (a) BFO, (b) BNF, (c) BFM, and (d) BNFM films grown on Pt coated (100)STO substrate. The rms values of surface roughness of films are shown in the inlet of figures.

BFO film, and thus improvement of the surface roughness (R_{rms}) was observed. It might be caused by a rise in crystallization temperature due to rare-earth element substitution.[15] In case of BFM film, the grain size was increased to approximately 500 to 1000 nm in size, which was two times lager than that in the BFO film. The R_{rms} value in the BFM film was 19 nm, and it was not appreciably reduced because of some porous parts between the grains. In the BNFM film, the some grains with similar size of those in the BNF film were observed. Besides, very small grains (less than 50 nm) were densely packed in plain area than that of BNF film, which looks like to constitute the large aggregate with flat surface, and thus the quite smooth surface morphology was formed as shown in the figure. In fact, the R_{rms} value of the BNFM film was also slightly smaller than that of the BNF film. Hence, these findings suggest that both of the features in BNF and BFM films are transferred to the BNFM film since the formation of large aggregates and the improvement of surface roughness are realized in the film.

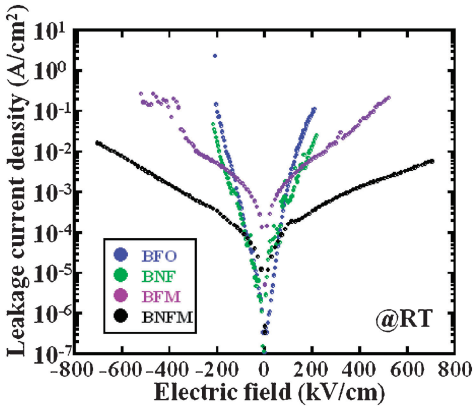

Fig. 3. Leakage current density vs electrical field curves for BFO, BNF, BFM, and BNFM film capacitors measured at room temperature.

In order to identify the influences of different dopants, the leakage current properties of BFO, BNF, BFM, and BNFM film capacitors were measured and shown in Fig. 3. The BFO and BNF films show low leakage current in the low electric field region (<100 kV/cm). However, the leakage current increase rapidly with an increase in the applied electric field and we could not measure them due to current limit of measurement system above 200 kV/cm. Additionally, the leakage current of BNF film was slightly lower than that of BFO film. It is not only arisen from improvement of crystallinity and surface morphology but also suppression of oxygen vacancies and valence fluctuation of Fe ions in the film by the Nd-substitution.[11] In the BFM film, although the leakage current density is higher than that in the BFO and BNF films in the low bias region, it can be kept on the order of 10^{-2} A/cm^2 at 400 kV/cm and breakdown property of the film is improved as shown in the figure. Singh *et al.* reported a same behavior of leakage current properties in the Mn-doped BFO films and they explained that improved characteristic was mainly caused by densely packed large size grains of internal structure of film from TEM observation.[7] Although we have not observed the internal structure of films, similar phenomena might be expected in our Mn-doped specimens. In contrast, in the BNFM film, both of reduced leakage current in low bias region and improved breakdown property are observed similar to BNF and BFM films, respectively. As a result, the BNFM film shows much lower leakage current density than other films in a wide range of electric field (100 to 700 kV/cm^2). Also, it is considered the reduced leakage current in the BNFM film by the two orders of magnitude compared with the BFM film is mainly caused by Nd doping effects such as smooth surface morphology and suppression of various defects in the film. Therefore, we regard the origin of reduced leakage current in the BNFM film in a wide range of electric field is synergetic effect of "suppression of impurity phases, oxygen vacancies and valence fluctuations of Fe ions" and "smooth surface morphology and densely packed grain structure" by the Nd and Mn codoping.

Figures 4(a) and 4(b) show the polarization vs electric field (P–E) curves of BFM and BNFM film capacitors, respectively. The P–E curves were measured at RT with a measurement frequency of 100 Hz. Here, in the BFO and

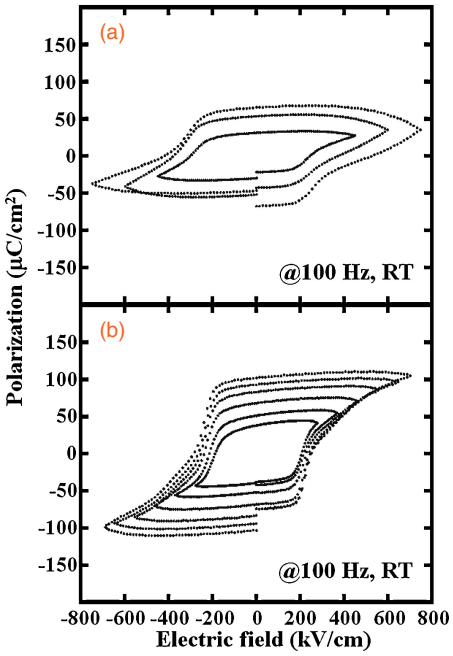

Fig. 4. Polarization vs electrical field loops of (a) BFM and (b) BNFM film capacitors measured at room temperature with measurement frequency of 100 Hz.

BNF film, no P–E curves could be observed because of their high leakage current. For the BFM film, the hysteresis loops were changed to distorted curve with increasing the electric field (>500 kV/cm). On the other hand, in case for the BNFM film, hysteresis loops were observed as shown in the figure, although the rounding of curves due to leakage current was remained. This difference of behavior is caused by the difference in magnitude of leakage currents in the high bias region. In general, higher measurement frequency than 1 kHz is required to measure the P–E curve in the BFO films because of low resistivity of the resistor components of the BFO grains and grain boundaries in the film.[6] Hence, the stable P–E curve in the BNFM film measured at 100 Hz means that those resistor components in the film have high resistivity even at RT.

Figure 5 shows the electric field dependence of remanent polarization P_r and coercive field E_c in the BNFM film capacitor. P_r and E_c at a maximum electric field of 700 kV/cm were approximately 100 μC/cm^2 and 250 kV/cm, respectively. Although the influences of leakage current (especially on P_r value) can not be neglected, these values are roughly comparable with those of polycrystalline BFO film capacitors obtained by optimizing the process conditions in detail.[3,4] It is supposed the (Nd,Mn)-codoping in the BFO film is effective technique resulting the ferroelectric properties without serious degradations due to the ion substitution. In addition, to reveal the advantages of (Nd,Mn)-codoping technique, further investigations are required by using improved method such as P–E curve measurement with higher frequency sweeping which depress the influences of leakage current.

In summary, we prepared the (Nd,Mn)-codoped BFO thin films on Pt/STO substrate by PLD and investigated

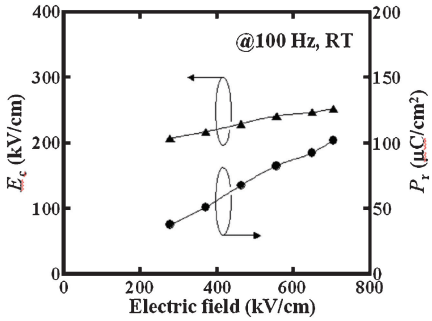

Fig. 5. Electrical field dependence of remanent polarization and coercive field measured at room temperature with measurement frequency of 100 Hz for BNFM film capacitor.

the influences due to codoping on crystallinity, surface morphology and electrical properties of the films. The XRD analysis and AFM observation indicated that both of suppression of impurity phases and smooth surface morphology were realized in the BNFM film. The BNFM film showed lower leakage current density than that of BFO, BNF, and BFM films in a wide range of electric fields. The P–E hysteresis curves were observed with measurement frequency of 100 Hz at RT. P_r and E_c for maximum electric field of 700 kV/cm were approximately 100 μC/cm^2 and 250 kV/cm, respectively.

Acknowledgment The authors would like to thank Professors M. Kumeda and K. Sasaki for fruitful discussions and S. Shiomoto, Y. Sakaguchi, and Y. Kurata for their technical supports.

1) J. Wang, J. B. Neaton, H. Zheng, V. Nagarajan, S. B. Ogale, B. Liu, D. Viehland, V. Vaithyanathan, D. G. Schlom, U. V. Waghmare, N. A. Spaldin, K. M. Rabe, M. Wuttig, and R. Ramesh: Science **299** (2003) 1719.
2) J. Wang, H. Zheng, Z. Ma, S. Prasertchoug, M. Wuttig, R. Droopad, J. Yu, K. Eisenbeiser, and R. Ramesh: Appl. Phys. Lett. **85** (2004) 2574.
3) K. Y. Yun, D. Ricinschi, T. Kanashima, and M. Okuyama: Appl. Phys. Lett. **89** (2006) 192902.
4) S. K. Singh and H. Ishiwara: Jpn. J. Appl. Phys. **44** (2005) L734.
5) K. Y. Yun, M. Noda, M. Okuyama, H. Saeki, H. Tabata, and K. Saito: J. Appl. Phys. **96** (2004) 3399.
6) H. Y. Go, N. Wakiya, H. Funakubo, K. Satoh, M. Kondo, J. S. Cross, K. Maruyama, N. Mizutani, and K. Shinozaki: Jpn. J. Appl. Phys. **46** (2007) 3491.
7) S. K. Singh, H. Ishiwara, and K. Maruyama: Appl. Phys. Lett. **88** (2006) 262908.
8) H. Uchida, R. Ueno, H. Funakubo, and S. Koda: Jpn. J. Appl. Phys. **44** (2005) L561.
9) Y. H. Lee, J. M. Wu, and C. H. Lai: Appl. Phys. Lett. **88** (2006) 042903.
10) Y. P. Liu and J. M. Wu: Electrochem. Solid-State. Lett. **10** (2007) G39.
11) F. Huang, X. Lu, W. Lin, X. Wu, Y. Kan, and J. Zhu: Appl. Phys. Lett. **89** (2006) 242914.
12) J. K. Kim, S. S. Kim, W. J. Kim, A. Bhalla, and R. Guo: Appl. Phys. Lett. **88** (2006) 132901.
13) X. Qi, J. Dho, R. Tomov, M. Blamire, and J. L. MacManus-Driscoll: Appl. Phys. Lett. **86** (2005) 062903.
14) S. K. Singh, K. Maruyama, and H. Ishiwara: Appl. Phys. Lett. **91** (2007) 112913.
15) C. C. Lee and J. M. Wu: Electrochem. Solid-State. Lett. **10** (2007) G58.